

Raising Bi-O Bands above the Fermi Energy Level of Hole-Doped $\text{Bi}_2\text{Sr}_2\text{CaCu}_2\text{O}_{8+\delta}$ and Other Cuprate Superconductors

Hsin Lin, S. Sahrakorpi, R. S. Markiewicz, and A. Bansil

Physics Department, Northeastern University, Boston, Massachusetts 02115, USA

(Received 1 June 2005; published 6 March 2006)

The Fermi surface (FS) of $\text{Bi}_2\text{Sr}_2\text{CaCu}_2\text{O}_{8+\delta}$ (Bi2212) predicted by band theory displays Bi-related pockets around the $(\pi, 0)$ point, which have never been observed experimentally. We show that when the effects of hole doping either by substituting Pb for Bi or by adding excess O in Bi2212 are included, the Bi-O bands are lifted above the Fermi energy (E_F) and the resulting first-principles FS is in remarkable accord with measurements. With decreasing hole doping the Bi-O bands drop below E_F and the system self-dopes below a critical hole concentration. Computations on other Bi- as well as Tl- and Hg-based compounds indicate that lifting of the cation-derived band with hole doping is a general property of the electronic structures of the cuprates.

DOI: [10.1103/PhysRevLett.96.097001](https://doi.org/10.1103/PhysRevLett.96.097001)

PACS numbers: 74.72.Hs, 71.18.+y, 74.25.Jb, 74.72.-h

First-principles band theory computations on the cuprates have become a widely accepted tool for gaining insight into their electronic structures, spectral properties, Fermi surfaces (FS's), and as a starting point for constructing theoretical models for incorporating strong correlation effects beyond the framework of the local-density approximation (LDA) underlying such calculations [1–4]. For example, in the double layer Bi compound $\text{Bi}_2\text{Sr}_2\text{CaCu}_2\text{O}_{8+\delta}$ (Bi2212)—perhaps the most widely investigated cuprate—the LDA generated band structure [5,6] is commonly invoked to describe the doped metallic state of the system. Band theory however clearly predicts the FS of Bi2212 to contain a FS pocket around the antinodal point $M(\pi, 0)$ as a Bi-O band drops below the Fermi energy (E_F), but such FS pockets have never been observed experimentally [7]. This “Bi-O pocket problem” is quite pervasive and occurs in other Bi compounds [8]. Similarly, Tl and Hg compounds display cation-derived FS pockets, presenting a fundamental challenge for addressing on a first-principles basis issues related to the doping dependencies of the electronic structures of the cuprates.

In this Letter, we show how the cation-derived band responsible for the aforementioned FS pockets is lifted above E_F when hole-doping effects are properly included in the computations. Detailed results for the case of Bi2212 are presented, where hole doping is generated either by substituting Pb for Bi or by adding excess oxygen in the Bi-O planes. With 20% Pb doping in the orthorhombic crystal structure, the Bi-O band lies ≈ 1 eV above E_F and the remaining bonding and antibonding FS sheets are in remarkable accord with the angle-resolved photoemission (ARPES) measurements on an overdoped Bi2212 single crystal [9]. Below a critical hole-doping level, the Bi-O band falls below E_F and, as a result of this self-doping effect, further reduction in the hole-doping level no longer reduces the number of holes in the CuO_2 layers. We argue that the underlying mechanism at play here is that hole doping reduces the effective positive charge in the Bi-O

donor layers, which then reduces the tendency of the electrons to “flow back” and self-dope the material. We have also carried out computations on a number of related compounds, including monolayer and trilayer Bi-compounds [$\text{Bi}_2\text{Sr}_2\text{CaCu}_2\text{O}_{6+\delta}$ (Bi2201) and $\text{Bi}_2\text{Sr}_2\text{CaCu}_2\text{O}_{10+\delta}$ (Bi2223)], and the Tl- and Hg-based compounds, and we find that the lifting of the cation-derived band with hole doping is a generic property of many families of cuprates.

Concerning technical details, we have employed both the Korringa-Kohn-Rostoker (KKR) and linearized augmented plane wave (LAPW) band structure methodologies where we treat all electrons in the system self-consistently and consider the full crystal potential without the muffin-tin approximation [10,11]. The KKR scheme is well known to be particularly suited for a first-principles treatment of the electronic structure of substitutionally disordered alloys. Pb substitution on the Bi sites was considered within the framework of the virtual crystal approximation (VCA), where the Bi nuclear charge Z is replaced by the average of the Bi and Pb charges of what may be thought of as an “effective” Bi/Pb atom, but otherwise the band structure problem is solved fully self-consistently maintaining the charge neutrality of the system. The VCA is expected to be a good approximation in this case since the effective disorder parameter for the Bi-O states, given by Δ/W , where Δ is the splitting of the Bi-O and Pb-O bands in Bi2212 and Pb2212, respectively, and W is the bandwidth, is estimated to be ~ 0.3 , so that the system is far from being in the split-band limit [12]. We have also carried out superlattice computations by substituting Bi atoms by Pb at two sites in the orthorhombic Bi2212 as well as KKR-coherent potential approximation (KKR-CPA) computations [10] in 10% Pb-doped Bi2201 to independently verify that the VCA provides a good description and that Bi/Pb substitution causes little disorder induced smearing of states.

We set the stage for our discussion by considering Fig. 1(a) which shows the band structure of undoped Bi2212 predicted by the LDA. Here the lattice is assumed

to be tetragonal and the structural parameters used are those of Ref. [6], obtained by minimizing the total energy. A pair of closely placed bands is seen to disperse rapidly through E_F along the Γ - $X(\pi, \pi)$ line on the right side of Fig. 1(a). These are the well-known CuO_2 bands which are split into bonding and antibonding combinations due to intracell interactions between the two CuO_2 planes. The problem however is that additional bands of Bi-O character drop below E_F at the $M(\pi, 0)$ point giving the so-called “Bi-O pockets,” leading to a metallic Bi-O layer, [13] in clear disagreement with experimental observations [7].

Figure 1(b) shows how the band structure changes dramatically around the M point when 25% Pb is substituted for Bi in Bi2212, where the band structure of the doped compound is computed within the VCA [14]. The Bi-O pocket problem is cured as the Bi-O bands are lifted to ≈ 0.4 eV above E_F , and the band structure around the M point is simplified and the bilayer splitting of the CuO_2 bands around M becomes more clearly visible. The extended van Hove singularities (VHSs) in the antibonding and bonding bands appear at binding energies of -0.07 and -0.45 eV, respectively, and the bare bilayer splitting at M is ≈ 400 meV. The shape of the antibonding and bonding CuO_2 bands is very similar to the generally accepted shape in the cuprates. The bands in Fig. 1(b) closely resemble the bands obtained in previous computations [3,15] where an *ad hoc* modification of the LDA potential was invoked to account for the absence of Bi-O pockets in the ARPES spectra of Bi2212. Further computations for a range of Pb-doping levels indicate that the Bi-O pockets are lifted just above E_F at around 22% Pb doping in the tetragonal structure.

The crystal structure of Bi2212 is more realistically modeled as a $\sqrt{2} \times \sqrt{2}$ orthorhombic unit cell [16]. Accordingly, Fig. 2 delineates the effect of doping in orthorhom-

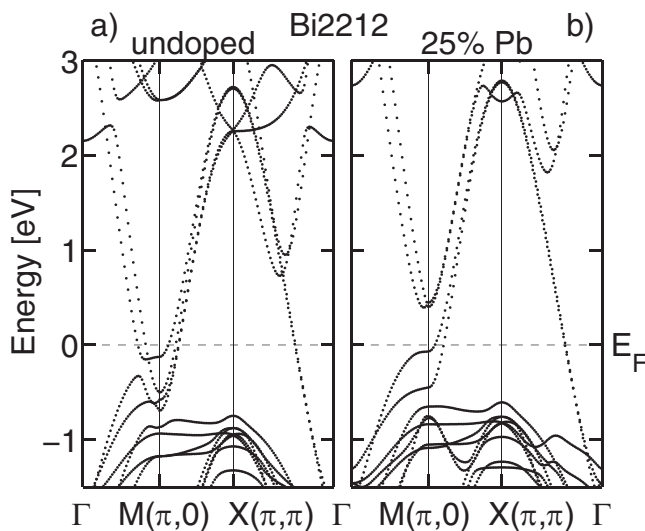


FIG. 1. Band structure of undoped and 25% Pb-doped tetragonal Bi2212 along various high symmetry directions at $k_z = 0$.

bic Bi2212 [6,17,18]. Here one obtains twice the number of bands compared to tetragonal Bi2212 due to the larger size of the unit cell. Comparing Figs. 2(a) and 2(b) we see that 15% Pb doping in the orthorhombic case lifts the Bi-O pockets ≈ 0.4 eV above E_F and yields a FS consisting of only the bonding and antibonding CuO_2 sheets.

A comparison of Figs. 1 and 2 reveals interesting differences between the band structures of tetragonal and orthorhombic Bi2212 and their evolution with Pb doping. The Bi-O complex of bands is more spread out in energy in Fig. 2(a) than in Fig. 1(a), which reflects the larger atomic displacements in Bi-O layers in the orthorhombic structure. The Bi-O bands display greater sensitivity to Pb doping in the orthorhombic case and only 12% Pb doping pushes the Bi-O pockets above E_F compared to the value of 22% needed in the tetragonal structure. There also are differences in the CuO_2 bands. For example, the doping level at which the VHS of the antibonding band lies at the E_F is 22% in the orthorhombic structure and 27% in the tetragonal case. Besides the highly dispersive CuO_2 bands, the complex of Cu-O bands below E_F [starting around a binding energy of ≈ 0.8 eV in Fig. 2(a)], which is primarily composed of Cu d and O p bands, is also influenced by the crystal structure and doping as seen with reference to Figs. 1 and 2. In particular, in the doped orthorhombic system in Fig. 2(b), around the M point, these lower lying bands mix significantly with the CuO_2 band involved in producing the bonding FS sheet, and change the shape of the associated VHS.

Figure 3 shows that our theoretically predicted FS is in remarkable accord with the experimentally determined FS of an overdoped Bi2212 sample obtained via ARPES measurements [9]. For this purpose, computed FS contours

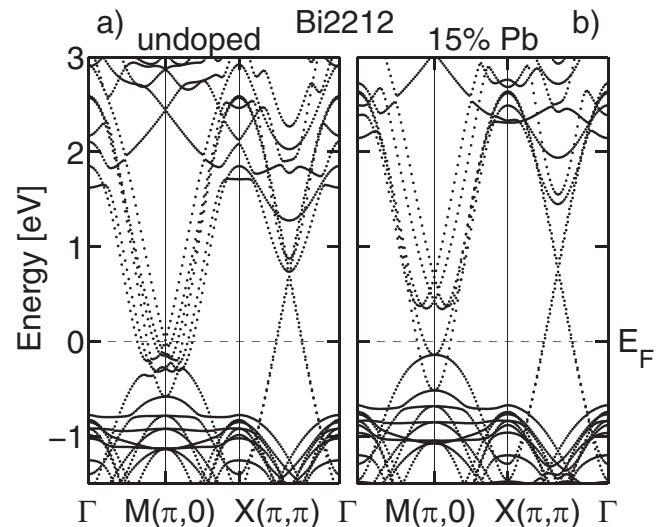


FIG. 2. Band structure (at $k_z = 0$) of undoped and 15% Pb-doped Bi2212 assuming orthorhombic lattice structure. Bands are plotted along the high symmetry lines of the tetragonal lattice for ease of comparison with the results of Fig. 1.

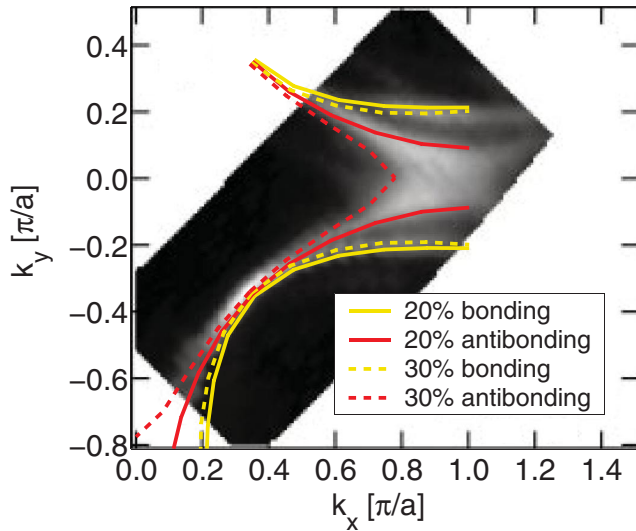


FIG. 3 (color). Theoretical bonding (yellow lines) and antibonding (red lines) FS's of orthorhombic Bi2212 for 20% (solid lines) and 30% (dashed lines) Pb doping. Other shadow FS's are not shown for simplicity. Experimental FS map taken via ARPES from an overdoped single crystal of Bi2212 is from Ref. [9].

for Pb-doping levels of 20% (solid lines) and 30% (dashed lines) for the orthorhombic lattice are overlaid on the experimental FS map [19–21]. The “shadow” FS's in the computations are not shown in order to highlight the main bonding and antibonding FS's. The computed bonding FS (yellow lines) shows relatively little change over 20%–30% doping range and its shape and dimensions are in quantitative accord with measurements. The antibonding FS (red lines), on the other hand, is more sensitive to doping and changes from being holelike at 20% doping (solid red line) to turning electronlike (dashed red line) at 30% doping as the E_F descends through the VHS. Therefore the spectral intensity associated with the antibonding FS in the antinodal region will be sensitive to local variations in hole doping and a careful modeling of the spectral intensities will be required to pin down details of the FS. However, along the nodal direction, neither the antibonding nor the bonding FS is sensitive to doping and here there is good accord between theory and experiment.

The driving mechanism underlying the lifting of the Bi-O pockets with Pb doping in our computations may be understood as follows. The ionization of Bi atoms in the system will in general generate electric fields which tend to attract electrons back into the Bi-O layers and compete with the affinity for the electrons towards the CuO_2 layers. The band structures of Fig. 1(a) or Fig. 2(a), which display partially filled Bi-O bands and the associated Bi-O pockets at the FS, then imply that the balance of forces in the computations is such that Bi is not fully ionized to $3+$ in pure Bi2212 so that we may think of some of the Bi^{3+} electrons as being attracted back to the Bi-O layers or

that the CuO_2 layers are self-doped with holes. The fact that the Bi-O bands are moved above E_F with Pb doping in Fig. 1(b) or Fig. 2(b) then indicates that the substitution of Bi with Pb and the concomitant reduction of positive charge in the Bi-O layers eliminates the need for electrons to flow back to the Bi-O layer. In effect then at, e.g., 25% Pb doping an empty (Bi/Pb)-O band only donates 0.75 rather than 1.0 electron to the CuO_2 layer. It is helpful as well to see how this argument plays out in reverse, i.e., with decreasing Pb doping. When Pb doping decreases, the tendency of the Bi/Pb electrons to flow back to the (Bi/Pb)-O layer increases and below a critical Pb-doping level some of the Bi/Pb electrons actually flow back as the (Bi/Pb)-O band drops below E_F . As a result of this self-doping effect, a further decrease in hole doping of the CuO_2 layers is prevented.

We turn now to consider the effect of adding excess O in Pb-free Bi2212 for hole doping the system. For this purpose, we have carried out extensive computations where O, F, or other pseudoatoms are inserted in the empty spaces between the Bi-O layers in order to capture varying amounts of Bi electrons to form a closed shell [22]. Typical modifications in the band structure are shown in Fig. 4, where we see that the effect of excess O is to lift the Bi-O pockets much like that of Pb/Bi substitution. The key is to reduce the effective number of electrons available in the Bi-O layers for donation to the CuO_2 layers and this can be accomplished via either Pb/Bi substitution or by adding excess O [23–25]. In Fig. 4, the Bi-O pockets lie below E_F for excess O value of $\delta = 0.1$, but lie well above E_F for $\delta = 0.3$. Our analysis indicates that the Bi-O pockets move through the E_F at $\delta \approx 0.18$.

We have also considered the effect of hole doping on other Bi compounds and find that the Bi-O bands in the

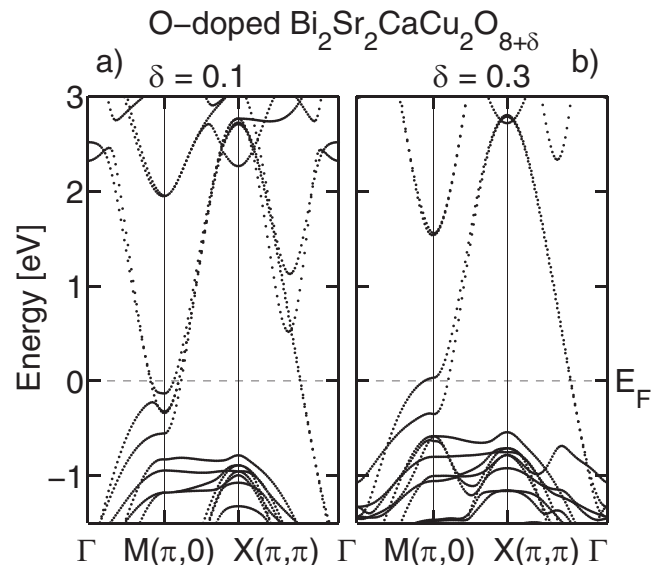


FIG. 4. Band structures of O-doped Bi2212: (a) $\delta = 0.1$, and (b) $\delta = 0.3$, where δ denotes excess O per unit cell.

15% Pb-doped Bi2201 and Bi2223 are lifted above E_F , even though the band structures of the undoped compounds in both cases display Bi-O FS pockets [26–28]. Going beyond the Bi compounds, we have studied doping effects on the band structures and binding energies of the core levels [29,30] in the Tl- and Hg-based cuprates. In particular, the Tl-O pockets around Γ point in Tl-based cuprates are removed by approximately 10% hole doping [31]. Interestingly, in $\text{Tl}_2\text{Ba}_2\text{CuO}_6$ (Tl2201), inclusion of hole doping results in a 3D FS that agrees well with the angular magnetoresistance oscillation measurements of Ref. [32]. The Hg-derived bands in the Hg-based cuprates are similarly lifted by O doping.

In order to assess the effect of superlattice modulation, we have carried out a series of computations in the orthorhombic structure where the refined parameters of Miles *et al.* [18] at various positions along the modulation were used. We found that the Bi-O pockets could not be lifted for any value of the parameters [6,33]. Even otherwise, we would not expect superlattice modulation to provide a generic mechanism for lifting the cation-derived bands in the cuprates because these modulations vary greatly between different cuprates, and are suppressed by Pb doping in the Bi compounds.

In conclusion, our results show clearly that substantial and generic Coulombic effects come into play with hole doping to lift the cation-derived bands in the cuprates. In adducing various physical quantities from spectroscopic data (e.g., the size of the pseudogap), changes in the electronic structure with underdoping, especially near the antinodal point, should be accounted for, even though most of the existing analysis in the cuprate literature assumes a doping-independent band structure. Finally, our study provides a first-principles route for exploring self-doping effects and doping dependencies of the electronic structures of this exciting class of materials.

We are grateful to S. Kaprzyk for important discussions and technical help and thank Z.-X. Shen for bringing Ref. [30] to our attention. This work is supported by the U.S. DOE Contract No. DE-AC03-76SF00098, and benefited from the allocation of supercomputer time at the NERSC and Northeastern University's Advanced Scientific Computation Center (ASCC).

-
- [1] W. E. Pickett, *Rev. Mod. Phys.* **61**, 433 (1989).
 - [2] E. Pavarini *et al.*, *Phys. Rev. Lett.* **87**, 047003 (2001).
 - [3] A. Bansil and M. Lindroos, *Phys. Rev. Lett.* **83**, 5154 (1999).
 - [4] R. S. Markiewicz *et al.*, *Phys. Rev. B* **72**, 054519 (2005).
 - [5] M. S. Hybertsen and L. F. Mattheiss, *Phys. Rev. Lett.* **60**, 1661 (1988).
 - [6] V. Bellini *et al.*, *Phys. Rev. B* **69**, 184508 (2004).
 - [7] A. Damascelli *et al.*, *Rev. Mod. Phys.* **75**, 473 (2003).

- [8] D. J. Singh and W. E. Pickett, *Phys. Rev. B* **51**, 3128 (1995).
- [9] P. V. Bogdanov *et al.*, *Phys. Rev. B* **64**, 180505(R) (2001).
- [10] A. Bansil *et al.*, *Phys. Rev. B* **60**, 13396 (1999).
- [11] P. Blaha *et al.*, *WIEN2k* (Tech. Univ., Vienna, 2001).
- [12] See, e.g., A. Bansil, *Phys. Rev. B* **20**, 4035 (1979).
- [13] Z. Zhang and C. M. Lieber, *Phys. Rev. B* **46**, R5845 (1992).
- [14] Z of the effective Bi atom is reduced from 83 to 82.75 to reflect the average charge of the Bi and Pb atoms.
- [15] M. Lindroos, S. Sahrakorpi, and A. Bansil, *Phys. Rev. B* **65**, 054514 (2002).
- [16] S. A. Sunshine *et al.*, *Phys. Rev. B* **38**, R893 (1988).
- [17] Optimized structural parameters for the orthorhombic lattice from Ref. [6] were used. Similar results are obtained if the experimental structure of Ref. [18] is used.
- [18] P. A. Miles *et al.*, *Physica C (Amsterdam)* **294**, 275 (1998).
- [19] The $k_z = 0$ sections of the FS are shown in Fig. 3 for simplicity. We will not be concerned here with issues of k_z dispersion and the resulting broadening of ARPES spectral lines as discussed in Refs. [20,21].
- [20] A. Bansil *et al.*, *Phys. Rev. B* **71**, 012503 (2005).
- [21] S. Sahrakorpi *et al.*, *Phys. Rev. Lett.* **95**, 157601 (2005).
- [22] An added O atom with $Z = 8$ ($\delta = 1.0$) captures two additional electrons/unit cell from the Bi-O layers to form a closed shell with $Z = 10$, while an F atom only takes away one electron corresponding to $\delta = 0.5$. A Ne atom ($Z = 10$) possesses a closed shell and we find it to have little effect on band structure. The values of δ in the results of Fig. 4 were simulated by adding two pseudoatoms/unit cell with $Z = 10 - \delta$. Very similar results are obtained if O atoms in Bi-O layers are replaced by pseudoatoms with Z less than 8.0, so that these atoms attract more than two electrons.
- [23] Interestingly, Pb solubility in Bi2212 is found to increase with decreasing O partial pressure, as suggested by these results (Refs. [24,25]).
- [24] P. Majewski, *J. Mater. Res.* **15**, 854 (2000).
- [25] J. MacManus-Driscoll and Z. Yi, *J. Am. Ceram. Soc.* **81**, 1322 (1998).
- [26] Since in Bi2212 the experimental and optimized lattice parameters give similar results in the orthorhombic case, we have used experimental orthorhombic parameters for Bi2201 and Bi2223 from Refs. [27,28], respectively.
- [27] C. C. Torardi *et al.*, *Phys. Rev. B* **38**, 225 (1988).
- [28] G. Miede *et al.*, *Physica C (Amsterdam)* **171**, 339 (1990).
- [29] We predict cation-related core levels (i.e., Bi, Tl, Hg, Sr, Ca) to move to lower binding energies with increasing hole doping. Measurements of Ref. [30] on the Tl $4f_{7/2}$ core level in a Tl compound are consistent with these predictions.
- [30] K. Tanaka *et al.*, *Phys. Rev. B* **63**, 064508 (2001).
- [31] See also M. Plate *et al.*, *Phys. Rev. Lett.* **95**, 077001 (2005).
- [32] N. E. Hussey *et al.*, *Nature (London)* **425**, 814 (2003).
- [33] In addition to structural distortions, surface effects could also play a role in lifting the Bi-O pockets above E_F . The analysis of Ref. [6], however, indicates that this is not the case.